PROGRESS IN INORGANIC CHEMISTRY

Edited by
STEPHEN J. LIPPARD

DEPARTMENT OF CHEMISTRY
COLUMBIA UNIVERSITY
NEW YORK, NEW YORK

VOLUME 23

AN INTERSCIENCE® PUBLICATION
JOHN WILEY & SONS, New York · London · Sydney · Toronto

Progress in
Inorganic Chemistry
Volume 23

Advisory Board

PROGRESS IN INORGANIC CHEMISTRY

Edited by
STEPHEN J. LIPPARD

DEPARTMENT OF CHEMISTRY
COLUMBIA UNIVERSITY
NEW YORK, NEW YORK

VOLUME 23

AN INTERSCIENCE® PUBLICATION
JOHN WILEY & SONS, New York · London · Sydney · Toronto

An Interscience® Publication

Library of Congress Catalog Card Number: 59–13035
ISBN 0–471–02186–5

Printed in the United States of America

10 9 8 7 6 5 4 3 2 1

Contents

Aspects of the Stereochemistry of Six-coordination

D. L. KEPERT

University of Western Australia
Nedlands, Western Australia

CONTENTS

I. INTRODUCTION

A. Scope of Review

This review centers on the stereochemical effect of introducing bidentate chelate rings into the coordination sphere of six-coordinate complexes. It seems hardly necessary to state that such complexes have occupied the central position in the development of coordination chemistry since the time of Werner. Experimental and theoretical results over the last five years, however, have significantly added to our understanding of this subject.

For many decades the usual starting point for any description of inorganic stereochemistry has been the *cis*- and *trans*-isomerism found in octahedral complexes, such as in complexes containing both bidentate and unidentate ligands of the general type $[M(bidentate)_2(unidentate)_2]^{x\pm}$ and of optical isomerism in octahedral complexes of the general type $[M(bidentate)_3]^{x\pm}$. It has recently become apparent that the reason that many such complexes are approximately octahedral is that the bidentate ligand forms five- or six-membered chelate rings with the metal atom, typical examples being the classical ligands ethylenediamine and acetylacetonate, respectively. The reason for the choice of such ligands has rested on considerations of complex stability rather than stereochemistry.

Recent calculations using an extraordinarily simple theoretical approach shows that considerable departures from octahedral stereochemistry are expected for bidentate ligands of different design. These predictions are in accord with experimental results. This review concentrates on the stereochemistry of the metal-coordination sphere and excludes secondary aspects such as the conformation of the chelate rings, which may nevertheless be relatively important for complexes containing multidentate chelating ligands.

The opportunity is taken to update and add many previously unpublished results and to correct earlier work on complexes of the general types $[M(bidentate)_3]^{x\pm}$ (127), $[M(bidentate)_2(unidentate)_2]^{x\pm}$ (129, 131), and $[M(bidentate)(unidentate)_4]^{x\pm}$ (155).

To restrict the scope even further and to focus attention on the primary coordination geometry rather than the secondary distortions that occur due to the presence of different types of donor atom bonded to the central atom, this review is generally limited to complexes containing not more than two chemically dissimilar donor atoms. For example, for complexes containing both unidentate and bidentate ligands, not only will all unidentate ligands be the same and all bidentate ligands also be the same, but both ends of each bidentate ligand will be the same. Detailed comparison of bond angles is generally only justified when all donor atoms are the same, as in tris(bidentate) complexes.

In order to appreciate the results of the stereochemical calculations, the general method of calculating the basic stereochemistries is summarized. It is important to remember that substantial assumptions are incorporated in the theoretical model and that this model bypasses much of the theoretical basis of chemical bonding that has been progressively developed over the last 50 years. Therefore, the model is often prematurely rejected by the chemist, and one purpose of this review is, to once again, demonstrate its utility.

Abbreviations of ligands are given at the end of this chapter, following the bibliography.

B. Theoretical Background

The stereochemical arrangement of any number of ligand donor atoms surrounding a central atom is obtained by minimization of the total repulsion energy U, obtained by summing over all donor atom-donor atom repulsions, u_{ij}. It is not critically important whether the repulsion is considered to arise largely from either the electron clouds of the donor atoms themselves or the electrons in the central atom-donor atom bonds, except of course for compounds considered to contain stereochemically active nonbonding pairs of electrons (e.g., see Sections II.D and III.E).

It is assumed that the interaction u_{ij} between any two donor atoms i and j (or, alternatively, between any two electron pairs i and j) is purely repulsive and proportional to some inverse power n of the distance d_{ij} between them. If all bond lengths are equal, that is, all donor atoms lie on the surface of a sphere of radius r, then the results can be expressed in the form

$$U = \sum_{ij} u_{ij} = \sum_{ij} a_n d_{ij}^{-n} = a_n X r^{-n} \quad (i > j) \tag{1}$$

where a_n is the proportionality constant and X the repulsion energy coefficient, which is a function of n and the geometry of the coordination polyhedron. The nature of the central atom is considered to play no part in determining the stereochemistry, either through preferred bonding directions or by shielding the donor atoms from each other. The sole role of the central atom is considered to be to hold the donor atoms onto the surface of the sphere.

The total repulsion energy U can also be divided into the repulsions V_i experienced by each of the donor atoms (or bonds), by dividing the repulsion between any pair of donor atoms (or bonds) equally between them as given in Eq. 2, where Y_i are the individual atom-repulsion coefficients.

$$V_i = \sum_i \frac{u_{ij}}{2} = a_n Y_i \tag{2}$$

The repulsion-energy coefficient X will increase as the coordination

TABLE I
Repulsion-energy Coefficients, X

Complex	Geometry	$n = 1$	$n = 6$	$n = 12$	Ref.
$[M(Unidentate)_2]$	linear	0.50	0.02	0.0002	
$[M(Unidentate)_3]$	triangular	1.73	0.11	0.004	
$[M(Unidentate)_4]$	tetrahedral	3.67	0.32	0.02	
$[M(Unidentate)_5]$	trigonal bipyramidal	6.47	0.88	0.10	(128)
$[M(Unidentate)_6]$	octahedral	9.99	1.55	0.19	
$[M(Unidentate)_7]$	various	14.45	3.23	0.75	(244)
$[M(Unidentate)_8]$	square antiprism	19.67	5.19	1.50	(21, 126)
$[M(Unidentate)_9]$	tricapped trigonal prism	25.76	8.11	3.13	(126)

number increases, with typical values of X for various coordination numbers using selected values of n, as shown in Table I. Lower repulsion-energy coefficients will, of course, be obtained for complexes containing chelate groups that hold the donor atoms in fixed position, particularly if they are close together.

The success of this theory demonstrates that these repulsion energies are very important in determining the stereochemistry, although the magnitude of these repulsion-energy coefficients in real energy units cannot be evaluated. Nevertheless, some order-of-magnitude guesses can be made. Assuming that the repulsive energy limits the attainment of ever-increasing coordination numbers due to the formation of additional metal-ligand bonds, the increment in repulsion energy, as the coordination number is increased, would theoretically be of the same order of magnitude as the additional metal–ligand bond energy (minus any decrease in the other metal–ligand bond energies due to the increase in coordination number). Thus, one unit of repulsion energy is worth something in the region of 100 to 1000 kjoule $mole^{-1}$. A similar guess regarding the order of magnitude can be made by comparison of calculated and experimental activation energies for intramolecular isomerization reactions.

It is found that the calculated repulsion-energy coefficients of compounds with known crystal structures are mostly within 0 to 0.2 energy units (i.e., within 0–20 kjoule $mole^{-1}$) from the calculated minima. This again appears reasonable when it is remembered that to a certain extent the ligands cushion the inner coordination sphere from the distortions arising from inter- and intramolecular interactions further out in the molecule, such as those due to crystal packing.

The most appropriate value of n in the repulsion law cannot be known exactly. Fortunately, the geometry corresponding to each minimum on the potential energy surface does not usually depend very much on the assumed value of n. In those few cases where the calculated geometry does depend on the assumed value of n (128), the best agreement with experiment is obtained

for $n \sim 6$ to 10. This appears very reasonable for repulsions between electron clouds. In this work the previous custom of quoting results for $n = 1$ (i.e., unrealistically assuming Coulombic repulsion between ligands considered as point charges), $n = 6$, and $n = 12$ is continued. The dependence of the calculated stereochemistry on the assumed value of n can usually be taken as a qualitative guide to the shallowness of that minimum, and the stereochemical parameters that are sensitive to n can be varied without radically altering the total repulsion energy.

It is assumed that each bonded bidentate ligand is sufficiently rigid that interaction between its donor atoms can be considered to be constant, and this interaction is, therefore, omitted when summing over all other donor atom–donor atom repulsions. Each bidentate ligand is imagined as being of fixed "normalized bite" b, which is defined as the distance between the donor atoms of the chelate divided by the metal–donor atom distance. The important result is that the predicted and found stereochemistries are very dependent on the normalized bite of the chelate, which to a large extent can be determined by the appropriate ligand design (Section II. G).

The extraordinary simplicity of this theory enables its use for structurally complicated molecules. The ability to predict new structures and rationalize known structures as a function of the normalized bite of the bidentate ligands is the important advance offered by this approach to stereochemistry. These successes cannot be achieved, or at least are very much more difficult to do so, using any theory that is purely metal-centered (e.g., valence bond, crystal field, ligand field, and molecular orbital).

The method of calculation involves the above very simple energy expressions coupled with elementary trigonometry. Each donor atom is imagined as being on the surface of a sphere of unit radius, its position being given by its spherical coordinates ϕ_i and θ_i. Three such coordinates are sufficient to specify the position of both ends of each bidentate ligand, as the fourth coordinate can be calculated from the other three plus the normalized bite b. Three of the angular coordinates can be fixed when defining the coordinate axes. Hence, there remain 9, 8, 7, and 6 angular variables for complexes of the type $[M(unidentate)_6]^{x\pm}$, $[M(bidentate)(unidentate)_4]^{x\pm}$, $[M(bidentate)_2(unidentate)_2]^{x\pm}$, and $[M(bidentate)_3]^{x\pm}$, respectively.

The distance d_{ij} between any two donor atoms i and j is given by Eq. 3.

$$d_{ij}^2 = 2 - 2\cos\phi_i\cos\phi_j - 2\sin\phi_i\sin\phi_j\cos(\theta_i - \theta_j) \qquad (3)$$

For the more general situation where the bond length to atom i is r_i and that to atom j is r_j, the appropriate equation is

$$d_{ij}^2 = (r_i - r_j)^2 + r_i r_j[2 - 2\cos\phi_i\cos\phi_j - 2\sin\phi_i\sin\phi_j\cos(\theta_i - \theta_j)] \qquad (4)$$

The calculation technique is simply to allow all angular coordinates to systematically vary until a minimum in the repulsion energy is reached.

II. TRIS(BIDENTATE LIGAND) COMPLEXES

A. The Theoretical Stereochemistry

Repulsion-energy calculations show that the stereochemistry corresponding to the single minimum on any potential energy surface always contains a threefold axis. The stereochemistry is, therefore, completely defined by the normalized bite of the bidentate ligand b and the angle of twist θ between

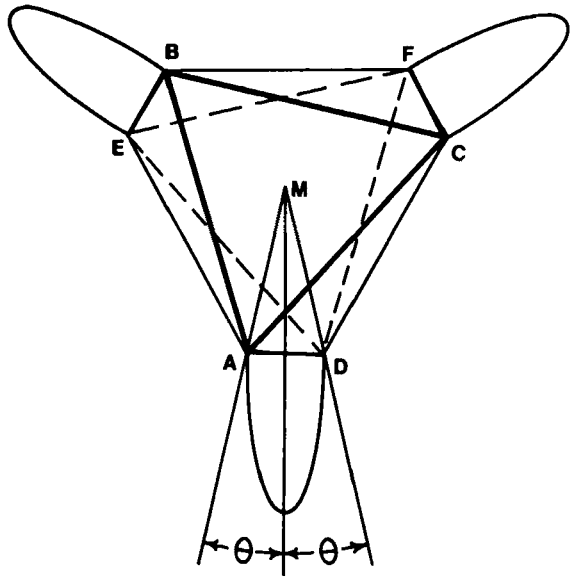

Fig. 1. General stereochemistry for $[M(bidentate)_3]^{x\pm}$.

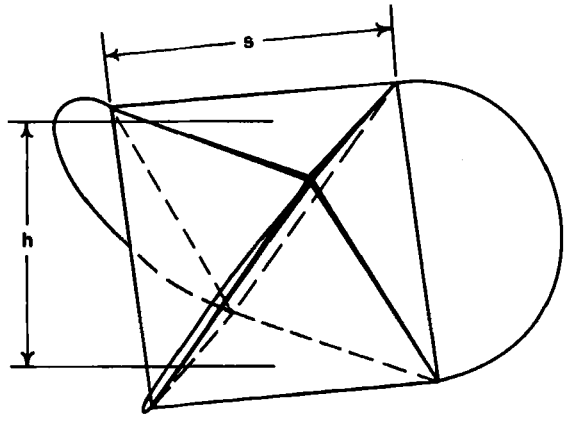

Fig. 2. Edge length s and height h for $[M(bidentate)_3]^{x\pm}$.

the upper and lower triangular faces (Fig. 1). The octahedron corresponds to the staggered arrangement with $\theta = 30°$, all octahedral edges being of equal length when $b = 2^{1/2}$. The trigonal prism is the eclipsed arrangement with $\theta = 0°$. (Other workers have alternatively chosen to define the polyhedron using the ratio s/h of the edge length s to the height h (Fig. 2). The relation between s/h and θ is given by:

$$\frac{s}{h} = \left(\frac{12 - 3b^2}{4b^2 - 16\sin^2\theta}\right)^{1/2}$$

For $b = 2^{1/2}$ and $\theta = 30°$, $s/h = 1.5^{3/2} = 1.22$).

The repulsion-energy coefficient X is shown as a function of the angle of twist θ and the normalized bite b (Fig. 3) for the particular case of $n = 6$. Similar curves are obtained using different values of n (127).

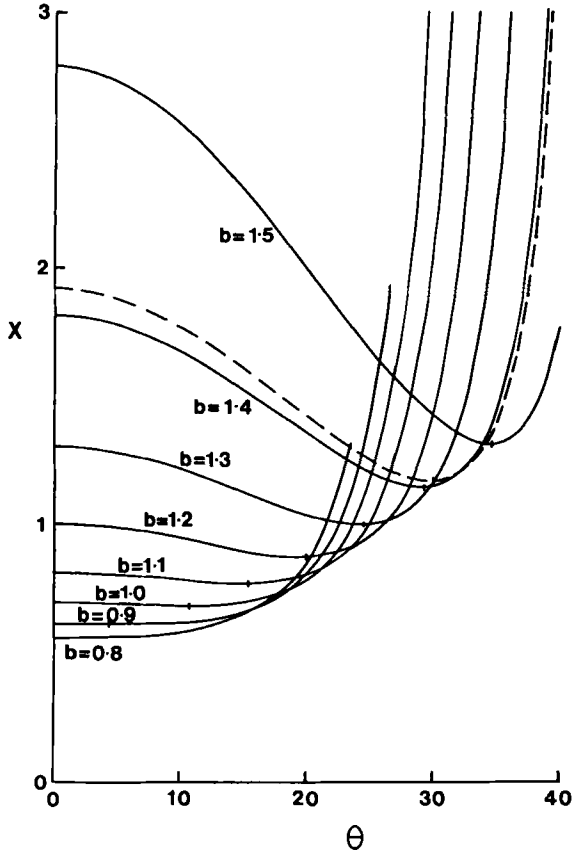

Fig. 3. Repulsion-energy coefficient X for $[M(bidentate)_3]^{x\pm}$ as function of angle of twist θ, ° and normalized bite b ($n = 6$); broken line corresponds to $b = 2^{1/2}$.

For normalized bites of $b = 2^{1/2} = 1.414$, the relatively deep energy minimum corresponds to the regular octahedron with $\theta = 30°$. The energy difference between this minimum and the maximum at $\theta = 0°$ is the activation energy for racemization of these optically active compounds by this simple twist mechanism and is examined in further detail in Section II.J.

As the normalized bite of the bidentate ligands is progressively decreased to 1.3 and 0.8, the upper triangular face *ABC* of the octahedron is brought into a more eclipsed configuration relative to the lower triangular face *DEF*, and the energy minimum moves to lower values of θ (Fig. 3).

The location of this minimum, θ_{min}, is plotted as a function of bidentate

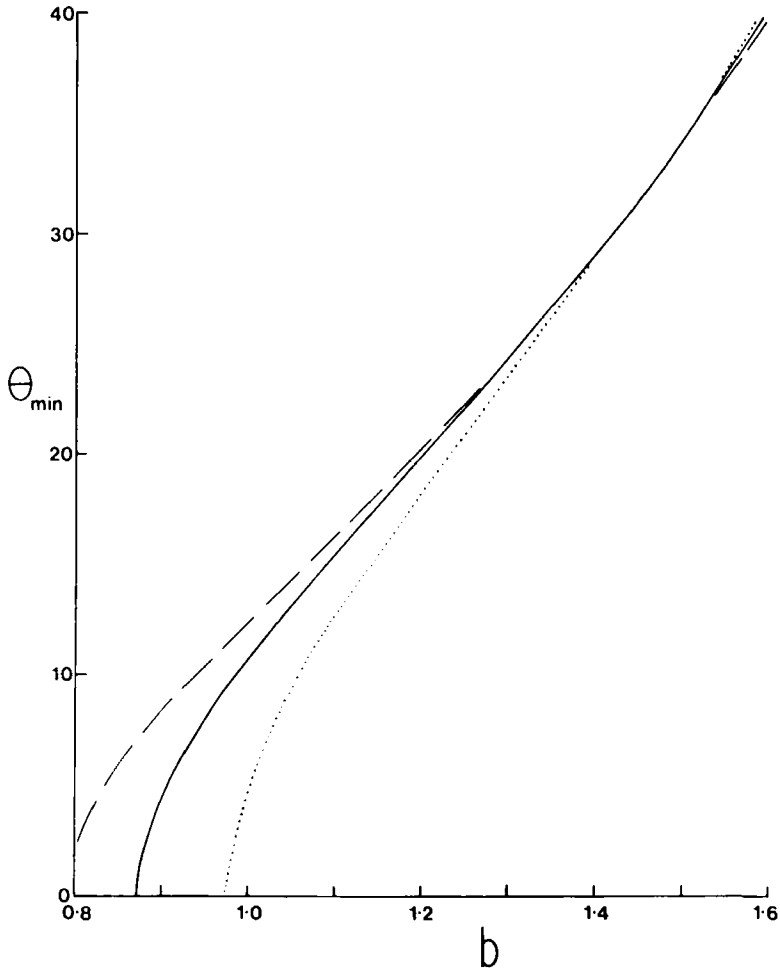

Fig. 4. Most stable stereochemistry, ° for $[M(bidentate)_3]^{x\pm}$ as function of normalized bite b: dotted line, $n = 1$; full line, $n = 6$; broken line, $n = 12$.

normalized bite in Fig. 4. Also shown are the minimum values assuming $n = 1$ and $n = 12$. The three theoretical curves cross at $b = 1.414$ and $\theta = 30°$.

The decrease in θ_{min} resulting from the decrease in b is accompanied by the potential-energy surface becoming much shallower in the vicinity of the minimum. This is illustrated in Fig. 5, which shows potential-energy contours ($n = 6$) for successive 0.01 energy units above the minimum and indicates generally how close real structures might be expected to conform to the calculated structures. This leveling of the potential energy surfaces also

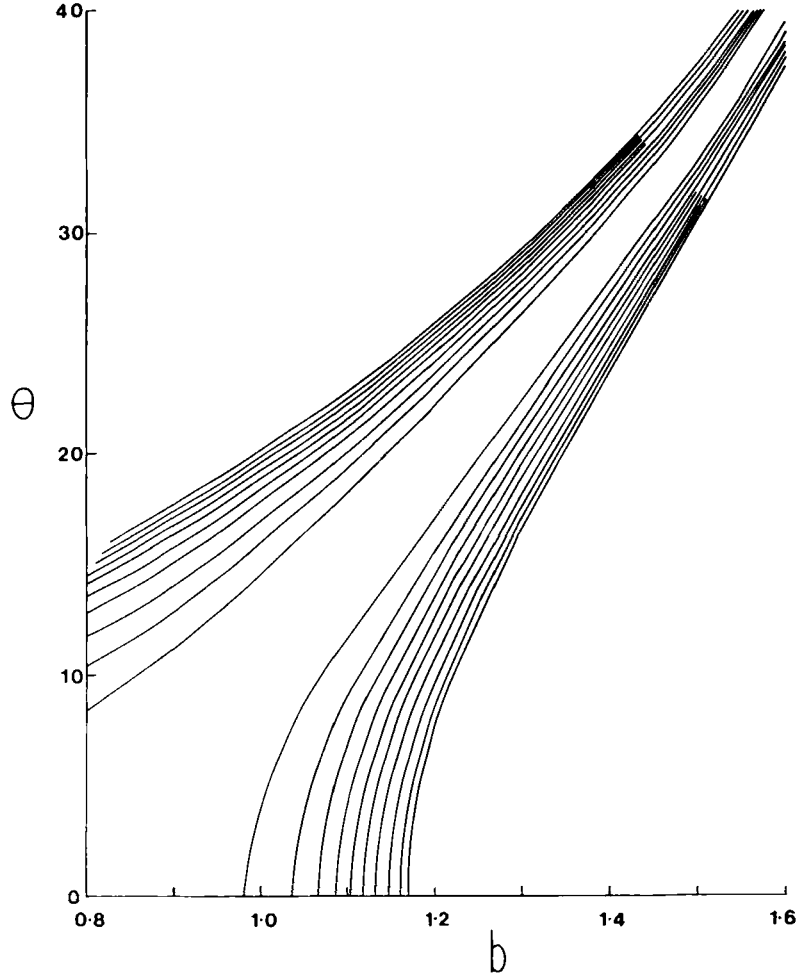

Fig. 5. Potential-energy contours for successive 0.01 increases in repulsion-energy coefficient X above the most stable stereochemistry for $[M(bidentate)_3]^{x\pm}$ ($n = 6$).

results in the precise location of the minimum being rather more dependent on the assumed value of n (Fig. 4).

B. Crystal Structures of 82 Complexes

Those molecules whose crystal structures have been described in sufficient detail to enable calculation of θ are listed in Table II. The structures of the majority conform reasonably well with the above predictions (Fig. 6). The errors in the structure determinations are not assessed, but it may be

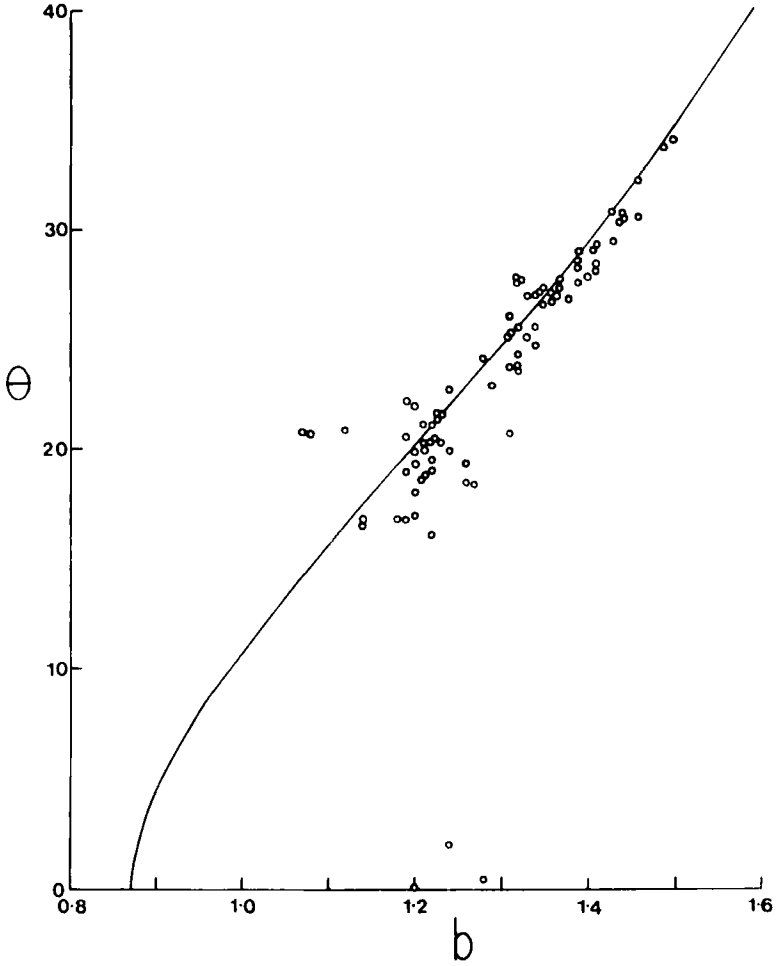

Fig. 6. Angle of twist θ, ° and normalized bite b for complexes of type $[M(bidentate)_3]^{x\pm}$; theoretical curve for $n = 6$ also shown.

noted that some of the cases where the agreement is less satisfactory are based only on preliminary reports of the crystal structure.

The three structures in Fig. 6 that deviate markedly from the theoretical curve are discussed in further detail in Section II.F. The following types of compound have been deleted from Table II and Fig. 6 at this stage: (1) complexes of manganese(III) and copper(II) (Section II.C), (2) complexes containing a stereochemically active lone pair of electrons (Section II.D), (3) dithiolate complexes (Section II.E), and (4) complexes containing grossly asymmetric chelate rings such as oxine (Section II.K). Chelate rings in which the donor atoms and the atoms immediately attached to them, are the same for both ends of the chelate have, however, been included; therefore, Table II and Fig. 6 include complexes of ligands such as propylenediamine, and xanthate.

TABLE II
Structural Parameters for $[M(bidentate)_3]^{x\pm}$

Complex	b	θ	Ref.
$[Co(acac)_3]$	1.50	34.0	(110)
	1.49	33.7	(141)
$[Ru(acac)_3]$	1.46	32.2	(41)
$[Fe(sacsac)_3]$	1.46	30.5	(17)
$[Ga(acac)_3]$	1.44	30.6	(56)
$[Al(acac)_3]$	1.44	30.4	(110)
$(NH_4)_2[Pt(S_5)_3]2H_2O$	1.44	30.3	(121)
$[Cr(acac)_3]$	1.43	30.8	(174)
(Et_3NH) $[P(o\text{-}C_6H_4O_2)_3]$	1.43	29.4	(3)
$[Co(bigu)_3]$	1.41	29.2	(237)
$[Cr(tn)_3]$ $[Ni(CN)_5]2H_2O$	1.41	29.0	(123)
$CaK[Co(S_2C_2O_2)_3]4H_2O$	1.41	28.5	(39)
$[Co(ten)_3]Br_3$	1.40	27.9	(222)
$[Co(ompp)_3](ClO_4)_2$	1.39	28.8	(120)
$[Co(en)_3]Br_3,H_2O$	1.39	28.5	(178)
$K[As(o\text{-}C_6H_4O_2)_3]1\frac{1}{2}H_2O$	1.39	27.5	(133)
$[Fe(acac)_3]AgClO_4,H_2O$	1.39	28.2	(181)
$[Fe(acac)_3]$	1.38	26.8	(119)
$[Mg(ompp)_3](ClO_4)_2$	1.37	27.7	(120)
$[Co(chxn)_3]Cl_3,5H_2O$	1.37	27.3	(154)
$[Co(pn)_3]Br_3$	1.36	27.1	(143)
$[Co(en)_3](NO_3)_3$	1.36	27.1	(256)
$[Co(en)_3](CdCl_6)Cl_2,2H_2O$	1.36	26.7	(250)
$[Co(en)_3][Cr(CN)_5(NO)]2H_2O$	1.35	27.3	(68)
$[(C_{14}H_{19}N_2)]$ $[Mg(hfac)_3]$	1.35	26.5	(245)
$[Co(pn)_3][Co(CN)_6]2H_2O$	1.34	27.0	(142)
$K[Ni(phen)_3][Co(C_2O_4)_3]2H_2O$ (anion)	1.34	27.0	(38)
$[Co(chxn)_3]Cl_3,H_2O$	1.34	25.5	(134)
$[Co\{S_2P(OMe)_2\}_3]$	1.34	24.7	(149)

TABLE II, (*cont.*)

Complex	b	θ	Ref.
$[Co(en)_3](Cu_2Cl_8)Cl_2,2H_2O$	1.33	26.9	(106)
$K_3[Cr(o\text{-}C_6H_4O_2)_3]1\frac{1}{2}H_2O$	1.33	25.2	(35)
$[Fe(phen)_3](ClO_4)_3,H_2O$	1.32	27.8	(12)
$[Fe(phen)_3](SbC_4O_6H_2)$	1.32	27.6	(258)
(bipyH) $[Fe(bipy)_3](ClO_4)_4$	1.32	27.6	(255)
$[Cr(en)_3][Ni(CN)_5]1\frac{1}{2}H_2O$	1.32	25.6	(215)
$[Al(trop)_3]$	1.32	24.3	(176)
$[Cr\{S_2P(OEt)_2\}_3]$	1.32	23.8	(227)
$[Al\{O_2C_2S_2Ag(PPh_3)_2\}_3]$	1.32	23.5	(107)
$[Ru(en)_3]Cl_3,3H_2O$	1.31	26.0	(202)
$[Cr(en)_3][Co(CN)_6]6H_2O$	1.31	25.2	(216)
$[Ni(en)_3](SO_4)$	1.31	25.2	(159)
$[Sc(acac)_3]$	1.31	23.7	(8)
$[V\{S_2P(OEt)_2\}_3]$	1.31	20.7	(80)
$K[Ni(phen)_3][Co(C_2O_4)_3]2H_2O$ (cation)	1.29	22.9	(38)
$[Ni(phen)_3][Mn(CO)_5]_2$	1.28	24.1	(79)
$K[Cd(acac)_3]H_2O$	1.28	0.4	(86)
$[W(OCH_2CH_2O)_3]$	1.27	18.4	(225)
$[Fe(trop)_3]$	1.26	19.3	(89)
$[Fe\{O_2C_2S_2Ag(PPh_3)_2\}_3]$	1.26	18.5	(107)
$Rb_2[Na(hfac)_3]$	1.24	2	(72)
$[Ni(S_2CNBu_2)_3]Br$	1.24	22.7	(71)
$[Fe(S_2COEt)_3]$	1.24	19.9	(253)
	1.22	20.5	(114)
$[Co(S_2CNEt_2)_3]$	1.23	21.8	(28,162)
$[Co(S_2COEt)_3]$	1.23	21.6	(163)
$[Co(S_2CNC_4H_8O)_3]CH_2Cl_2$	1.23	21.5	(98)
$[Fe(S_2CNEt_2)_3]$ 79°K	1.23	20.3	(145)
297°K	1.21	18.8	(145)
$[Fe(S_2CSBu)_3]$	1.22	21.1	(146)
$[Fe(S_2CNMePh)_3]$	1.22	20.4	(99)
$[Fe\{S_2CN(CH_2)_4\}_3](ClO_4)$	1.22	19.0	(153)
$[Mn\{S_2CN(CH_2)_5\}_3](ClO_4),CHCl_3$	1.22	19.5	(34)
$[Fe(O_2N_2Ph)_3]$	1.22	16.1	(249)
$[Cr(S_2CSEt)_3]$	1.21	21.1	(43,146a)
$[Cr(S_2COEt)_3]$	1.21	20.3	(164)
$[Fe(S_2CNBu_2)_3]C_6H_6$	1.21	20.1	(170)
$[Fe\{S_2CN(CH_2)_4\}_3]$	1.21	18.7	(99)
$[Rh(S_2CNEt_2)_3]$	1.20	22.1	(211)
$[Cr(S_2CNEt_2)_3]$	1.20	20.0	(214)
$[Ga(S_2CNEt_2)_3]$	1.20	19.4	(57)
$(BzPh_3P)_2[Fe\{S_2CC(CO_2Et)_2\}_3]$	1.20	18.0	(108)
$[Sc(trop)_3]$	1.20	17.0	(9)
$[Er(BuCOCHCOBu)_3]$	1.20	0.0	(251)
$[Ir(S_2CNEt_2)_3]$	1.19	22.3	(212)
$[Ru(S_2CNEt_2)_3]$	1.19	19.0	(205)
$[Ru(S_2CNBz_2)_3]$	1.19	20.7	(214)

TABLE II, (*cont.*)

Complex	b	θ	Ref.
$[Fe(S_2CNBu_2)_3]$	1.19	16.8	(113)
$[Fe(S_2CNC_4H_8O)_3]CH_2Cl_2$	1.18	16.8	(98)
$[In(S_2CNEt_2)_3]$	1.14	16.9	(57)
$[In\{S_2CN(CH_2)_5\}_3]$	1.14	16.5	(96)
$[Co(NO_3)_3]$	1.12	20.9	(104)
$[Co(PhN_3Ph)_3]PhMe$	1.08	20.7	(46)
$[Co(PhN_3Ph)_3]$	1.07	20.8	(140)

For molecules that do not possess a crystallographic threefold axis, the angle of twist depends to a small extent on the method of calculation. In this work the calculations are based on the quoted bond angles, averaged assuming a three fold axis. Some justification for this procedure is given in Section II.L, where molecules markedly departing from this condition are described. Using this averaging procedure:

$$\alpha = (AMD + BME + CMF)/3$$
$$\beta = (AME + BMF + CMD)/3$$
$$\gamma = (AMB + BMC + AMC + DME + EMF + DMF)/6$$
$$b = 2\sin(\alpha/2)$$
$$\theta = \arctan\left\{\frac{2}{3^{1/2}}\left[\frac{\cos(\beta/2)}{\cos(\alpha/2)} - 0.5\right]\right\}$$

and

$$\theta = \arccos\left[\frac{3^{1/2}\cos(\alpha/2)}{2\sin(\gamma/2)}\right]$$

The agreement between theory and experiment in Fig. 6 is reasonably satisfactory and clearly demonstrates that regular octahedral stereochemistry is not generally expected for tris(chelate) complexes. The conclusion that the stereochemistry depends mainly on the normalized bite of the bidentate ligand is important to many of the studies in complexes of this type.

The following sections extend this approach a little further and also concentrate on a number of exceptional cases where the stereochemistry is modified from the above predictions by a variety of other factors.

C. Manganese(III) and Copper(II) Complexes

High-spin manganese(III) and copper(II) complexes have been excluded from Table II, since experience with complexes containing unidentate ligands leads to the expectation that the octahedral stereochemistry will be distorted because of the Jahn–Teller effect (the electron configurations being $t_{2g}^3 e_g^1$ and $t_{2g}^6 e_g^3$, respectively). This distortion is quite different from that arising from steric constraints imposed by the bidentate ligands. It may be noted that the

lowering of symmetry from that of the perfectly regular octahedron, by trigonal twisting, does not remove the Jahn–Teller degeneracy.

If, as a rough approximation, any Jahn–Teller distortions are ignored and the bond angles are averaged assuming D_3 symmetry, then the values of b and θ (Table III) calculated as before are again in reasonable accord with the repulsion-energy calculations (Fig. 7).

The two simple types of Jahn–Teller distortion that might be expected are a tetragonal elongation arising from the additional e_g electron being in the d_{z^2} orbital, or a tetragonal flattening arising from the additional e_g electron being in the $d_{x^2-y^2}$ orbital. However, the type and extent of the distortion appears to be quite variable, and in some cases the small distortion attributable to the Jahn–Teller effect is somewhat obscured by the small distortions often arising from crystal packing forces. The complexes can be subdivided into the following types:

1. $[Cu(ompp)_3](ClO_4)_2$ and $[Cu(en)_3](SO_4)$: in these compounds the crystallographic symmetry is such as to enforce D_3 symmetry on the copper atoms. All copper–ligand bond lengths are equal, no Jahn–Teller effect being observed. Two alternative explanations can be presented, which postulate that: (a) although each static $[Cu(bidentate)_3]^{2+}$ ion is distorted, there is rapid oscillation between the three mutually perpendicular tetragonal distortions at each lattice site (i.e., a dynamic Jahn–Teller effect) and (b) there is a random orientation of the tetragonally distorted molecules over all sites in the crystal, leading to the observed averaged regular octahedral structure.

2. $(C_{14}H_{19}N_2)[Cu(hfac)_3]$, $[Cu(phen)_3](ClO_4)_2$, and $[Cu(HOCH_2CH_2OH)_3]SO_4$. In these compounds there is a fairly obvious tetragonal elongation of the octahedron, two *trans* bonds being 8 to 16% longer than the other four (Table III).

3. $[Mn(S_2CNEt_2)_3]$ and $[Mn(trop)_3]\frac{1}{4}$ PhMe. In the first compound there

TABLE III

Structural Parameters for $[M(bidentate)_3]^{x\pm}$ (M = Mn^{III}, Cu^{II})

Complex	b	θ	Relative Bond Lengths	Ref.
$[Mn(acac)_3]$	1.41	30.1	2(1.00) + 2(1.02) + 2(1.03)	(70)
$[Mn(trop)_3]\frac{1}{4}$PhMe	1.27	24.5	4(1.00) + 2(1.10)	(11)
			4(1.00) + 2(1.04)	
$[Mn(S_2CNEt_2)_3]$	1.19	20.1	4(1.00) + 2(1.06)	(100)
$[Cu(ommp)_3](ClO_4)_2$	1.41	30.6	2(1.00) + 2(1.03) + 2(1.04)	(167)
$[Cu(ompp)_3](ClO_4)_2$	1.39	29.0	6(1.00)	(120)
$(C_{14}H_{19}N_2)[Cu(hfac)_3]$	1.38	28.7	4(1.00) + 2(1.08)	(245)
$[Cu(en)_3](SO_4)$	1.30	24.5	6(1.00)	(48)
$[Cu(HOCH_2CH_2OH)_3](SO_4)$	1.30	—	4(1.00) + 2(1.16)	(10)
$[Cu(phen)_3](ClO_4)_2$	1.26	25.9	4(1.00) + 2(1.14)	(7)
$[Cu(bipy)_3](ClO_4)_2$	1.25	25.5	4(1.00) + 1(1.10) + 1(1.21)	(6)

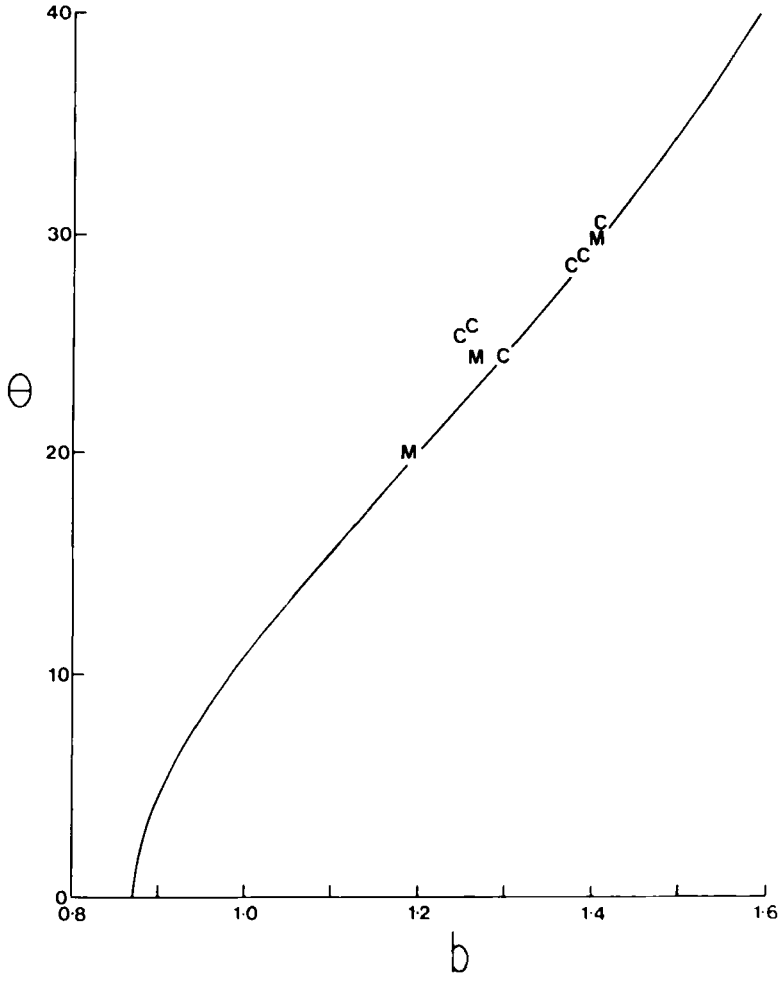

Fig. 7. Angle of twist θ, ° and normalized bite b for complexes of type $[Mn^{III}(bidentate)_3]^{x\pm}$ (M) and $[Cu^{II}(bidentate)_3]^{x\pm}$ (C); theoretical curve for $n = 6$ also shown.

is again a clear tetragonal elongation, two manganese–sulfur bonds being 6% longer than the other four. The compound is isomorphous with the rhodium analog, where all rhodium–sulfur distances are equal to within 1%. The tropolonate complex has two independent molecules in the unit cell with two significantly different degrees of tetragonal elongation (4% and 10%).

4. $[Cu(bipy)_3](ClO_4)_2$. In this case the two *trans* ligands are not pushed away equally, one bond being 10% and the other 21% longer than the other four bonds. This is not expected from the Jahn–Teller theorem.

5. $[Cu(ommp)_3](ClO_4)_2$ and $[Mn(acac)_3]$. In both of these complexes all three O—M—O units at right angles to each other have different metal–oxygen distances, resulting in orthorhombically distorted molecules. In both cases the distortion is closer to a tetragonal flattening rather than elongation of the octahedra.

In summary, the Jahn–Teller distortion observed in these $[M(bidentate)_3]^{x\pm}$ complexes is much less than that observed in $[M(unidentate)_6]^{x\pm}$ complexes, which may approach square planar structures. That is, the steric constraints imposed by bidentate ligands is more important than, and largely overcomes, the steric effects imposed by the electron configuration.

D. Complexes Containing a Lone Pair of Electrons

The dithiocarbamates $[As(S_2CNEt_2)_3]$ and $[Rh(S_2CNEt_2)_3]$ are isostructural (211). However, the presence of a stereochemically active lone pair of electrons lying along the threefold axis of the arsenic(III) complex is indicated by expansion of one of the triangular faces (S_b—As—S_b = 106°) relative to the other (S_a—As—S_a = 90°) (Fig. 8). The angles formed between the arsenic–sulfur bonds and the threefold axis are α = 67° and 55°, respectively. This distortion also introduces considerable asymmetry into the chelate rings, the arsenic–sulfur distances being 2.85 Å and 2.35 Å, respectively.

Similar distortions are observed in $[As(S_2COEt)_3]$ (40, 144), $[Sb(S_2COEt)_3]$ (84, 144), and $[Bi\{S_2P(OPr)_2\}_3]$ (144) (Table IV). These complexes are, therefore, best considered as having the seven-coordinate capped octahedral stereochemistry. The related compounds $(NH_4)_3[Sb(C_2O_4)_3]4H_2O$ (207) and $(Et_4N)[Pb(S_2COEt)_3]$ (177) are best considered as being based on other seven-coordinate geometries (130).

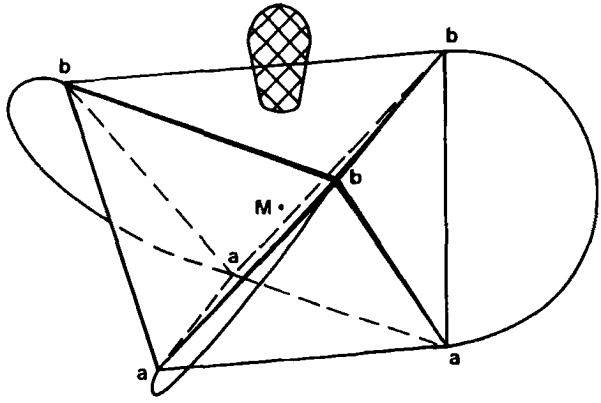

Fig. 8. $[M(bidentate)_3(lone\ pair)]^{x\pm}$.

TABLE IV
Structural Parameters of Tris(bidentate)(Lone Pair) Complexes

Complex	M—a	M—b	aMa	bMb	αa	αb
$[As(S_2CNEt_2)_3]$	2.35	2.85	90.1	106.0	54.8	67.2
$[As(S_2COEt)_3]$	2.28	2.94	92.0	107.6	56.2	68.7
$[Sb(S_2COEt)_3]$	2.52	3.00	87.5	113.1	53.0	74.5
$[Bi\{S_2P(OPr)_2\}_3]$	2.70	2.87	91.2	99.9	55.6	62.1

E. Dithiolate Complexes

Tris(bidentate) complexes based on ligands of the type

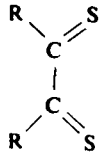

R = H, CN, Ph, CF_3

form complexes that are much further distorted away from the octahedron toward the trigonal prism than would be expected from simple repulsion-energy calculations. A second problem is the considerable difficulty in formulating these complexes, which may be described as either dithiolate or dithiolene:

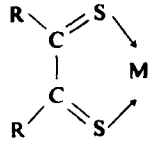

Dithiolene

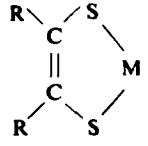

Dithiolate

The latter is obviously unrealistic for complexes such as $[V(S_2C_2Ph_2)_3]$, which would require the formation of vanadium(VI). Evidence from C—C and C—S bond lengths show that the bonding is intermediate between these extremes, indicating that there is extensive electron delocalization between the metal and ligands.

Similar complexes are formed with benzenedithiolate:

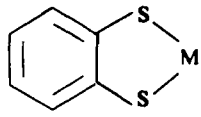

Calculated values of the normalized bite b and the twist angle θ for these complexes are given in Table V. The following observations may be made concerning the structures of these compounds:

TABLE V
Structural Parameters of Tris(dithiolate) Complexes

Complex	b	θ,°	Ref.
$(Ph_4As)_2[Fe\{S_2C_2(CN)_2\}_3]$	1.39	~24.5	(229)
$(Me_4N)_2[V\{S_2C_2(CN)_2\}_3]$	1.33	17.0	(241)
$[Mo(S_2C_2H_2)_3]$	1.33	0	(234)
$[Mo\{Se_2C_2(CF_3)_2\}_3]$	1.33	0	(204)
$(Ph_4As)_2[Mo\{S_2C_2(CN)_2\}_3]$	1.32	14.0	(32)
$(Ph_4As)_2[W\{S_2C_2(CN)_2\}_3]$	1.32	14.0	(32)
$[Mo(S_2C_6H_4)_3]$	1.31	0	(18)
$[V(S_2C_2Ph_2)_3]$	1.31	0	(61)
$[Re(S_2C_2Ph_2)_3]$	1.30	0	(62)
$(Ph_4As)[Ta(S_2C_6H_4)_3]$	1.30	~16.0	(152)
$(Ph_4As)[Nb(S_2C_6H_4)_3]$	1.29	0	(18)
$(Me_4N)_2[Zr(S_2C_6H_4)_3]$	1.28	~20.0	(18)

1. In sharp contrast to other tris(chelate) complexes, it is very clear that θ is not a simple function of b. In all cases θ is lower than predicted, and in many cases the trigonal prism with $\theta = 0°$ is observed. The stereochemistry closest to that expected from repulsion energy calculations is that of $[Fe\{S_2C_2(CN)_2\}_3]^{2-}$, for which $\theta = 24.5°$, compared with $\theta \sim 28°$, as expected for $b = 1.39$. These dithiolate ligands are clearly different from other bidentate ligands, even MeSCH=CHS$^-$, dithioacetylacetonate, dithiooxalate, dithiophosphates, dithiocarbamates, and xanthates (Table II).

2. Correlations between the twist angle and the choice of metal atom are rather tentative at this stage. Table VI plots the θ values against the number of electrons in the valence shell and the column in the periodic table.
a. The angle of twist appears to increase as the number of electrons in the valence shell increases. It is uncertain whether this is due to: (i) increasing occupancy of molecular orbitals that are antibonding with respect to form-

TABLE VI
Map of Twist Angles in Tris(dithiolate) Complexes

Number of electrons					
n		V ($\theta = 0°$)			
$n+1$	Zr^{2-}($\theta \sim 20°$)	Nb^-($\theta = 0°$) Ta^- ($\theta \sim 16°$)	Mo ($\theta = 0°$)		
$n+2$		V^{2-}($\theta = 17°$)		Re($\theta = 0°$)	
$n+3$			Mo^{2-}($\theta = 14°$) W^{2-}($\theta = 14°$)		
$n+4$					
$n+5$					Fe^{2-}($\theta = 25°$)

ing the trigonal prism, (ii) increasing charge on the complex making the ligand–ligand repulsions more important [note that all (2–) complexes are twisted], or (iii) other factors,

b. A substantial twist is observed in the $[Zr(S_2C_6H_4)_3]^{2-}$ complex, whereas the isoelectronic $[Nb(S_2C_6H_4)_3]^-$ and $[Mo(S_2C_6H_4)_3]$ complexes are trigonal prismatic.

3. Of all of these extraordinary structures, $(Ph_4As)[Ta(S_2C_6H_4)_3]$ is even more unusual in that there is only an extremely poor approximation to threefold symmetry. If a pseudothreefold axis is defined as being normal to the plane through the midpoint of each chelate, then individual twist angles for each chelate ring of 27°, 8°, and 8° can be calculated. As a result, the two triangular faces are no longer parallel, but inclined by 12°.

4. The twisting is associated with a number of other structural changes (Table VII), but whether these cause the twist (or vice versa) is again unclear. For example:

TABLE VII
Ligand Parameters (Å) of Tris(dithiolate) Complexes

Complex	θ,°	M—S	Intraligand S··S	Interligand S··S	S—C
$(Me_4N)_2[Zr(S_2C_6H_4)_3]$	~20	2.54	3.26	3.59	1.76
$(Ph_4As)[Nb(S_2C_6H_4)_3]$	0	2.44	3.15	3.23	1.74
$(Ph_4As)[Ta(S_2C_6H_4)_3]$	~16	2.43	3.15	~3.3	1.75
$[Mo(S_2C_6H_4)_3]$	0	2.37	3.11	3.09	1.73
$(Ph_4As)_2[Fe\{S_2C_2(CN)_2\}_3]$	24.5	2.26	3.12	3.21	1.73
$(Me_4N)_2[V\{S_2C_2(CN)_2\}_3]$	17.0	2.36	3.13	3.20	1.72
$(Ph_4As)_2[Mo\{S_2C_2(CN)_2\}_3]$	14.0	2.37	3.13	3.19	1.74
$(Ph_4As)_2[W\{S_2C_2(CN)_2\}_3]$	14.0	2.37	3.12	3.19	1.73
$[V(S_2C_2Ph_2)_3]$	0	2.34	3.06	3.06	1.69
$[Mo(S_2C_2Ph_2)_3]$	0	2.33	3.10	3.11	1.70
$[Re(S_2C_2Ph_2)_3]$	0	2.32	3.03	3.05	1.69
		M—Se	Se··Se	Se··Se	Se—C
$[Mo\{Se_2C_2(CF_3)_2\}_3]$	0	2.49	3.32	3.22	1.86

a. As the octahedron is twisted toward the trigonal prism, the S··S distance between the three ligands decreases. Bonding within these S_3 triangles, together with the utilization of metal *d*-orbitals, may well be important. Two such bonds may be visualized (242) (Fig. 9). The first arises from the remaining sp^2 hybrid (the other two being used for M—S and S—C σ-bonding) on each sulfur atom, and the metal d_{z^2} orbital projecting through the center of the S_3 face (Fig. 9*a*). The second arises from ligand(π) and the metal (d_{xy}, $d_{x^2-y^2}$) orbitals (Fig. 9*b*). Such bonding schemes would lead to both short intraligand S··S distances and short M–S bonds.

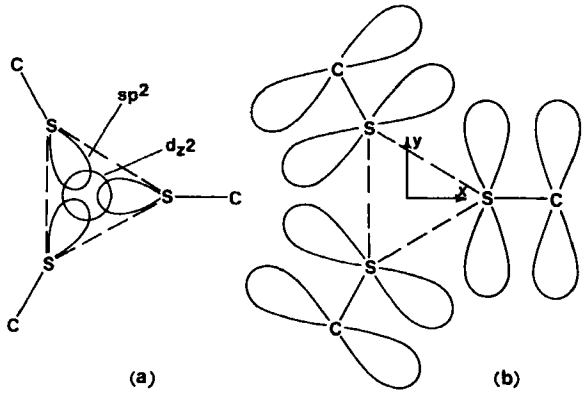

Fig. 9. Two types of sulfur–sulfur and metal–sulfur bonding in tris(dithiolate) complexes, viewed down threefold axis of trigonal prism.

b. Complexes closer to the trigonal prism appear to have shorter C—S bonds, suggesting an increased dithiolene contribution relative to the dithiolate contribution.

It is inappropriate to discuss these compounds any further, as they are clearly different to other tris(chelate) complexes.

F. Three Exceptional Structures

The following three compounds listed in Table II have angles of twist grossly at variance with predictions (Fig. 6), and it is necessary to seek other explanations for their structures:

$K[Cd(acac)_3]H_2O$	$b = 1.28$	$\theta = 0.4°$
$Rb_2[Na(hfac)_3]$	$b = 1.24$	$\theta = 2.°$
$[Er(Bu^tCOCHCOBu^t)_3]$	$b = 1.20$	$\theta = 0.0°$

In all cases three β-diketonate ligands are attached to large metal atoms, and the stereochemistry is virtually trigonal prismatic compared with expected angles of twist of $\theta \sim 24$ to 20°. Larger normalized bites are found in other structurally characterized tris(β-diketonate) complexes, and the structures are in accord with predictions. For example, the next largest normalized bite is bound for $[Sc(acac)_3]$ ($b = 1.31$), which has the normal structure ($\theta = 23.7°$).

It appears necessary to invoke extraordinary crystal-packing forces to explain the structure of the acetylacetonatocadmate complex. Three oxygen atoms of one triangular face of the CdO_6 trigonal prism are in contact with the potassium ion (K—O = 2.67–2.80 Å) (Fig. 10). Similarly, two oxygen

atoms of the other triangular face are in contact with another potassium ion (K—O = 2.76 Å and 2.80 Å), with the formation of an infinite linear polymer (Fig. 10). Any twist toward octahedral geometry must enlarge these triangular faces, with a possible weakening of the potassium—oxygen bonding.

In the erbium complex, however (Fig. 11), it may be that the large bulk

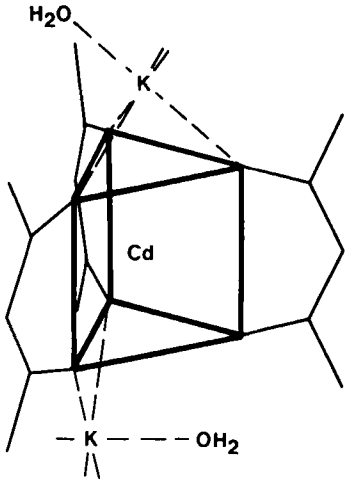

Fig. 10. $K[Cd(acac)_3]H_2O$.

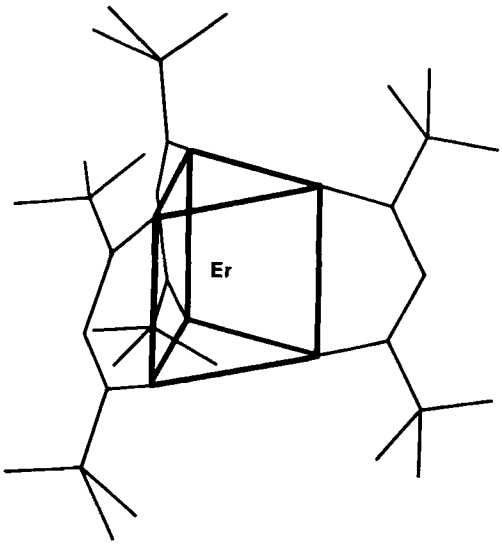

Fig. 11. $[Er(Bu^tCOCHCOBu^t)_3]$.

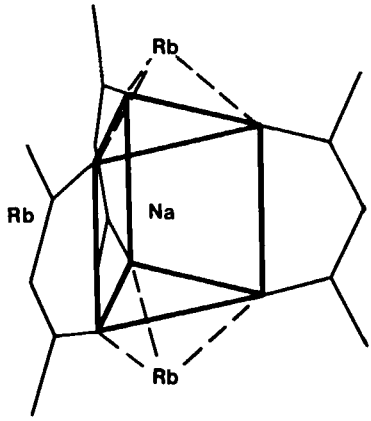

Fig. 12. $Rb_2[Na(hfac)_3]$.

of the tertiary butyl groups result in considerable intramolecular steric hindrance and prevent the complex twisting toward the octahedron.

Either or both of these explanations can be advanced for the structure of the hexafluoroacetylacetonatosodate complex. Rubidium ions again lie outside each of the triangular faces (Rb—O = 2.84–3.03 Å) and also outside one of the rectangular faces (Rb—O = 3.00–3.64 Å) (Fig. 12). The bulk of the trifluoromethyl groups may also be significant.

Clearly, additional work on charged and/or bulky β-diketonato complexes using large metal atoms would be of considerable interest.

G. Some Comments on Ligand Design

If the only way of obtaining the normalized bite of a coordinated bidentate ligand were from the crystal structure, the repulsion-energy approach to stereochemistry would be limited. No matter how useful the theory may be in rationalizing the relation between different stereochemical parameters, it would have little predictive use since these other stereochemical parameters are precisely determined at the same time as the normalized bite. Therefore, in order to fully utilize this repulsion approach to stereochemistry, it is essential to be able to make some estimate of the expected normalized bite of any coordinated ligand.

Figure 13 again displays some of the data contained in Tables II and III and Figs. 6 and 7. The data are now restricted to transition-metal complexes to avoid large variations in central atom size, but now include complexes of manganese(III) and copper(II).

To a first approximation the ligands divide into three groups. The first

group is contained within the limits $b = 1.37_5$ to $b = 1.50$ and consists of those ligands that form six-membered chelate rings such as acetylacetonate and trimethylenediamine. The second group is contained within the limits $b = 1.25$ to $b = 1.37_5$ and contains the complexes with five-membered chelate rings such as *o*-phenanthroline and ethylenediamine. The third group is contained within $b = 1.05$ to $b = 1.25$ and contains the complexes with four-membered rings such as the nitrates and dithiocarbamates. This strikingly simple and important correlation is further illustrated in Fig. 14 with three representative examples: $[Co(acac)_3]$, $[Co(en)_3]^{3+}$, and $[Co(NO_3)_3]$.

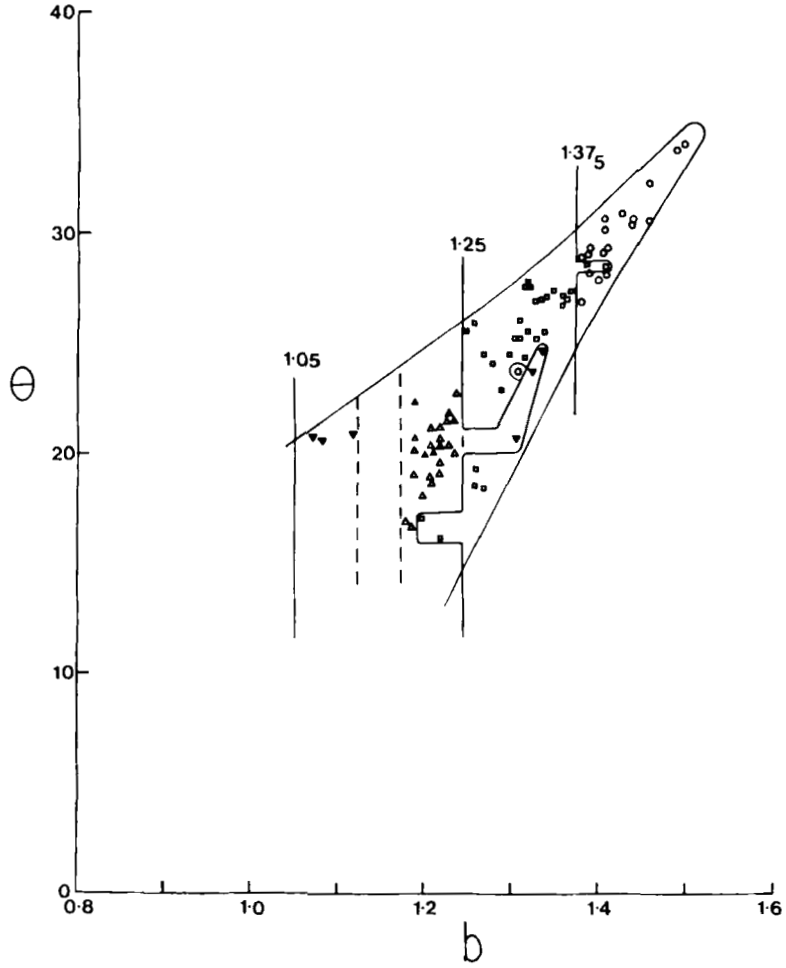

Fig. 13. Angle of twist θ, ° and normalized bite b for transition-metal complexes of type $[M(bidentate)_3]^{x\pm}$.

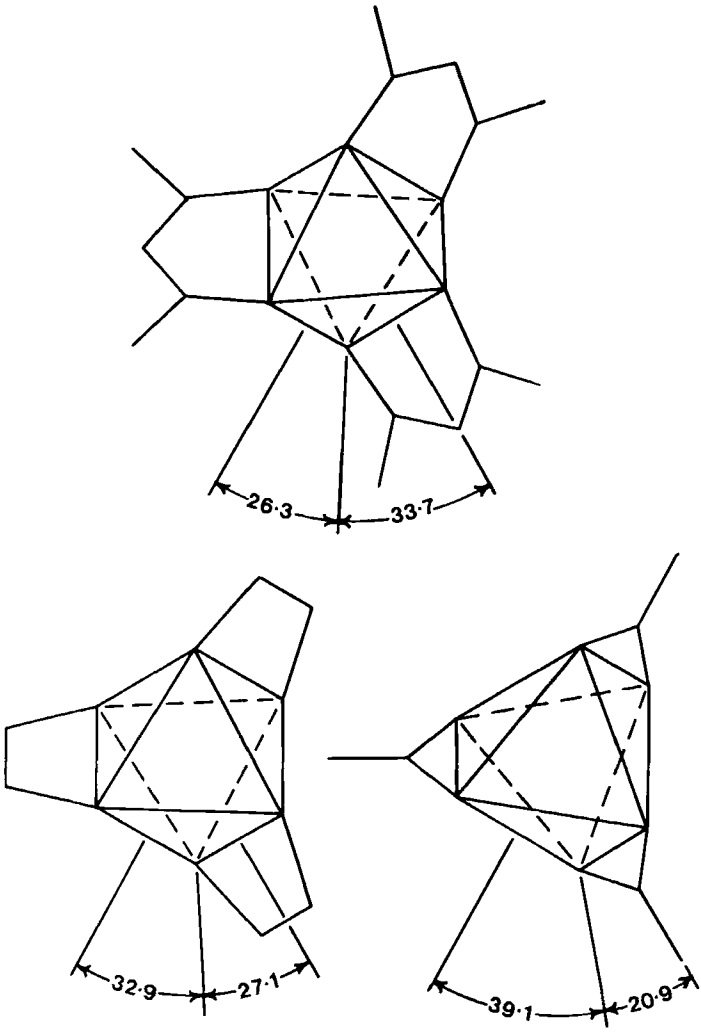

Fig. 14. $[Co(acac)_3]$, $[Co(en)_3]^{3+}$, and $[Co(NO_3)_3]$; angles, °.

Extension to flexible seven-membered rings does not necessarily increase the normalized bite, as indicated by the tetramethylenediamine complex $[Co(ten)_3]Br_3$, for which the parameters are $b = 1.40$ and $\theta = 27.9°$. This is achieved by substantial buckling of the seven-membered chelate ring.

The normalized bite is a function of the metal–ligand bond length, the smaller normalized bites being obtained with the larger metal atoms. Thus,

the lowest normalized bite for a six-membered ring shown in Fig. 13 is that observed for [Sc(acac)$_3$], in which the normalized bite of 1.31 is similar to complexes of the other transition metals containing five-membered chelate rings. Similarly, the lowest normalized bite for a five-membered ring in Fig. 13 is $b = 1.20$ observed for [Sc(trop)$_3$].

The metal–oxygen distance and the O··O intraligand distance are not completely independent of each other, as illustrated for example by the β-diketonate complexes listed in Table VIII. An increase in the metal ion radius of about 10% causes a general loosening of the coordination sphere, with a small increase of about 2 to 5% in the O··O distance. Similar correlations are readily observed for other classes of ligands in Table II. The specific case of iron dithiocarbamates is again referred to in Section II.H.

Conversely, very small central atoms will confer unusually large normalized bites on the chelated ligand, as is illustrated for three catecholate complexes in Table VIII. It is for these reasons that Fig. 13 was restricted to transition-metal complexes.

It was seen above that to a first approximation the bidentate ligands could be divided into three groups, depending on whether a six-, five-, or four-membered chelate ring was formed. A further subdivision can be made according to the size of the nonmetal atoms in the chelate ring. For example, the four-membered chelate ring group may be divided into four subgroups. The subgroup containing ligands of lowest normalized bite ($b = 1.05$–1.12_5) consists of $(PhN_3Ph)^-$ and NO_3^-, where three small second-row elements complete the chelate ring. There are no known examples of the second sub-

TABLE VIII
Structural Parameters of Tris(β-diketonate) and Tris(catecholate) Complexes

Complex	M—O	O··O	O—M—O	b	θ
$Rb_2[Na(hfac)_3]$	2.35	2.92	77	1.24	2
$K[Cd(acac)_3]H_2O$	2.28	2.92	79.5	1.28	0.4
[Er(BuCOCHCOBu)$_3$]	2.21	2.67	74.4	1.20	0.0
$(C_{14}H_{19}N_2)[Mg(hfac)_3]$	2.07	2.86	87.6	1.35	26.5
[Sc(acac)$_3$]	2.07	2.72	82.0	1.31	23.7
[Ru(acac)$_3$]	2.00	2.91	93.7	1.46	32.2
$[Fe(acac)_3]AgClO_4,H_2O$	2.00	2.78	88.0	1.39	28.2
[Fe(acac)$_3$]	1.99	2.74	87.1	1.38	26.8
[Ga(acac)$_3$]	1.95	2.80	91.8	1.44	30.6
[Cr(acac)$_3$]	1.95	2.79	91.1	1.43	30.8
[Co(acac)$_3$]	1.89	2.82	96.5	1.49	33.7
[Al(acac)$_3$]	1.89	2.72	91.9	1.44	30.4
$K_3[Cr(o\text{-}C_6H_4O_2)_3]$	1.99	2.65	83.6	1.33	25.2
$K[As(o\text{-}C_6H_4O_2)_3]$	1.84	2.57	88.2	1.39	27.5
$(Et_3NH)[P(o\text{-}C_6H_4O_2)_3]$	1.72	2.45	91.4	1.43	29.4

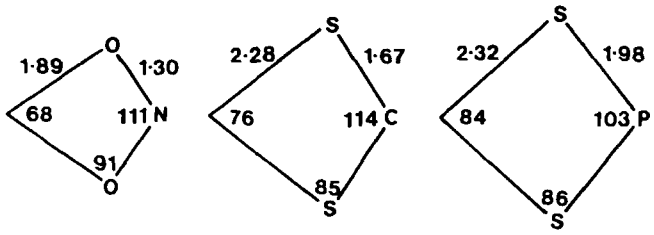

Fig. 15. Ring geometries, ° and Å, in $[Co(NO_3)_3]$, $[Co(S_2COEt)_3]$ and $[Co\{S_2P(OMe)_2\}_3]$.

group. The third subgroup of normalized bite $b = 1.17_5$ to 1.25 contains ligands with one second-row element and two larger elements in the chelate ring, such as the dithiocarbamates and xanthates. The fourth subgroup contains the dithiophosphates with three large ring atoms, and this subgroup intrudes into the group containing the five-membered chelate rings. A comparison of the ring geometries of $[Co(NO_3)_3]$, $[Co(S_2COEt)_3]$, and $[Co\{S_2P(OMe)_2\}_3]$ is shown in Fig. 15.

The smallest normalized bite for a four-membered chelate ring that can be envisaged is probably the borohydride ion. Although crystal structure data are not available, the electron-diffraction data of gaseous $[Al(BH_4)_3]$ have been interpreted as showing approximately trigonal prismatic coordination of three bidentate borohydride groups, $b = 1.20$, $\theta \sim 0°$ (4).

The increase in normalized bite on incorporating larger atoms into five-membered chelate rings will depend on the number of larger atoms and their position in the chelate ring. Rings completely formed from large atoms will have normalized bites typical of six-membered rings, as in $[Mo(PMe_2 \cdot AsMe \cdot AsMe \cdot PMe_2)(CO)_4]$, $b = 1.40$ (230).

Six-membered chelate rings will probably incorporate larger atoms by puckering of the ring rather than by large increases in normalized bite, as observed in $(NH_4)_2[Pt(S_5)_3]2H_2O$.

H. Spin Crossover in Iron(III) Complexes

Iron(III) tris(dialkyldithiocarbamates) and closely related complexes such as the alkylxanthates and alkylthioxanthates

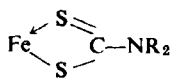

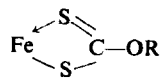

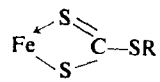

are well defined examples of a magnetic "crossover" situation. Assuming full O_h symmetry, the alternative electron configurations are low-spin t_{2g}^5 (ground state $^2T_{2g}$) and high-spin $t_{2g}^3\ e_g^2$ (ground-state $^6A_{1g}$). The energy

TABLE IX
Structural and Magnetic (69) Properties of Tris(dithiochelate)iron(III) Complexes

Complex		Fe—S	S··S	b	μ_{eff}	θ
$[Fe(S_2CNC_4H_8O)_3]CH_2Cl_2$		2.43	2.88	1.18	5.1	16.8
$[Fe(S_2CNBu^n_2)_3]$		2.42	2.87	1.19	5.3	16.8
$[Fe\{S_2CN(CH_2)_4\}_3]$		2.41	2.91	1.21	5.8	18.7
$[Fe(S_2CNEt_2)_3]$	297°K	2.36	2.85	1.21	4.2	18.8
$[Fe(S_2COEt)_3]$		2.34	2.87	1.24	2.7	19.9
		2.32	2.84	1.22	2.7	20.5
$[Fe(S_2CNMePh)_3]$		2.31	2.82	1.22	3.0	20.4
$[Fe(S_2CNEt_2)_3]$	79°K	2.31	2.84	1.23	2.2	20.3
$[Fe(S_2CSBu^t)_3]$		2.30	2.80	1.22	2.4	21.1

separation between these idealized ground states is of the order of kT, and the observed structure and properties are sensitive to the choice of alkyl substituent R and the temperature. The relative importance of each ground state is most easily determined by measuring the magnetic moment, being ~5.9 BM for a purely high-spin complex, and ~2.3 BM for a purely low-spin complex.

It would be expected that the Fe—S bond lengths in the high-spin complexes would be longer than in the low-spin complexes due to the electrons in the two e_g orbitals "pushing back" the sulfur atoms. Examination of a series of crystal structures (Table IX) shows that this difference amounts to ~0.1 Å. As expected, there is a direct correlation between decreasing Fe—S bond lengths and decreasing effective magnetic moment.

The decrease in Fe—S bond lengths leads to increased normalized bites of the bidentate ligands, which leads to increased values of θ, as expected (Table IX). (The increase in normalized bite is relatively small, as the de-decrease in Fe—S bond length is partially compensated by a decrease in S··S intraligand distance, due to a general increase in steric crowding on contraction of the FeS_6 core, as indicated in Section II.G.)

These features are illustrated in Table IX. Particularly striking are the differences between $[Fe(S_2CNEt_2)_3]$ at room temperature and at 79°K, where the decrease in Fe—S bond length and magnetic moment is accompanied by an increase in normalized bite of 0.02, and the 1.5° increase in the angle of twist θ is precisely that expected from ligand–ligand repulsion calculations.

I. Tris(alkene) Complexes

Minimization of the repulsion energy does not appear to be a valid approach to the stereochemistry of tris(alkene) complexes.

The palladium(O) complex *fac*-[Pd(PhCH:CHCOCH:CHPh)$_3$]C_6H_6 has the palladium atom bonded to one of the alkene units in each ligand:

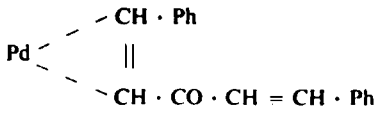

If the two carbon atoms are considered as the donor atoms of a bidentate ligand, the orientation of the carbon atoms are such that $b = 0.62$ and $\theta = 17°$ (160). In a preliminary communication, [Pt(bicyclo[2.2.1]heptene)$_3$] has been described as approximately planar ($b = 0.62$, $\theta \sim 36°$) (87). The bonding in these compounds is uncertain, and it may be noted that an 18-electron configuration is not reached if each ligand contributes only two electrons to the metal atom.

Similarly the bonding in *fac*-tris(methylvinylketone) tungsten

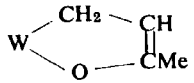

($b = 1.22$, $\theta = 0°$) is uncertain, and is grossly electron deficient if it is considered that each ligand behaves as a simple bidentate ligand (173).

J. Intramolecular Rearrangements

The two most plausible modes for the intramolecular racemization of the optically active tris-chelate complexes involve twisting of opposite triangular faces of the octahedron in opposite directions. The first such reaction (Fig. 16*a*) involves a trigonal twist about the C_3-axis, with the formation of a trigonal prismatic transition state where the bidentate ligands span the three parallel edges. The potential energy curves in Fig. 3 (Section II.A) correspond to the reaction coordinates for this type of reaction. The second mechanism (Fig. 16*b*) involves a trigonal twist about one of the pseudo-C_3-axes, in which the stereochemistry of the transition state is a trigonal prism with two of the bidentate ligands spanning triangular edges.

The relative energy of these two transition-state trigonal prisms will depend on the value of the normalized bite. In both transition states the upper bidentate ligands in Fig. 17 can be considered to lie above a rectangle formed by the donor atoms of the other two bidentate ligands. In the first case the upper bidentate ligand is projected above the rectangular edges between the other two bidentate ligands, whereas in the second case the upper bidentate ligand is projected above the other two bidentate ligands. These features are emphasized in the projections shown in Figs. 17*a* and 17*b*, respectively. For bidentate ligands with normalized bites below ap-

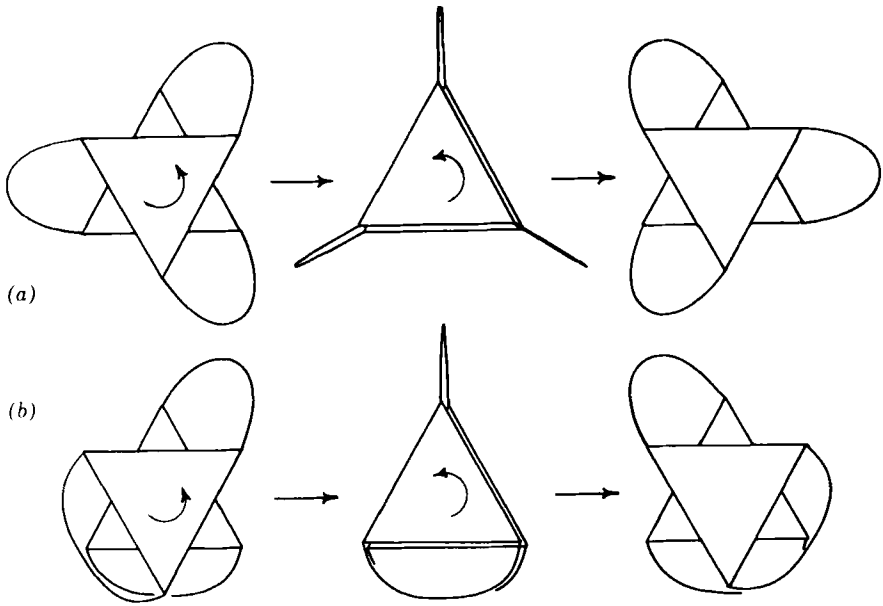

Fig. 16. Racemization of tris(bidentate) complexes: (*a*) twist about the C_3-axis; (*b*) twist about a pseudo-C_3-axis.

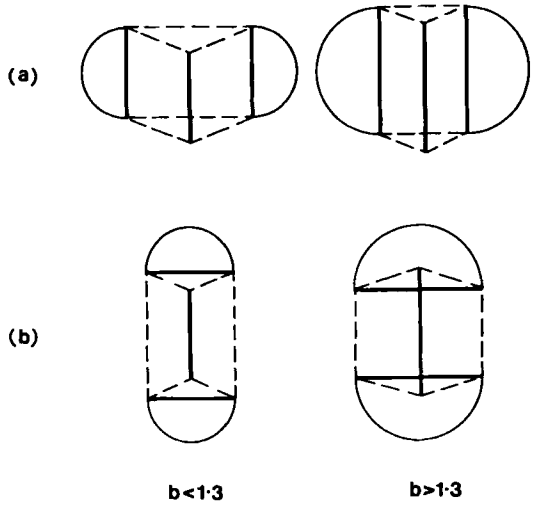

Fig. 17. Transition states for racemization of tris(bidentate) complexes: (*a*) twist about the C_3-axis; (*b*) twist about a pseudo-*C*-axis.

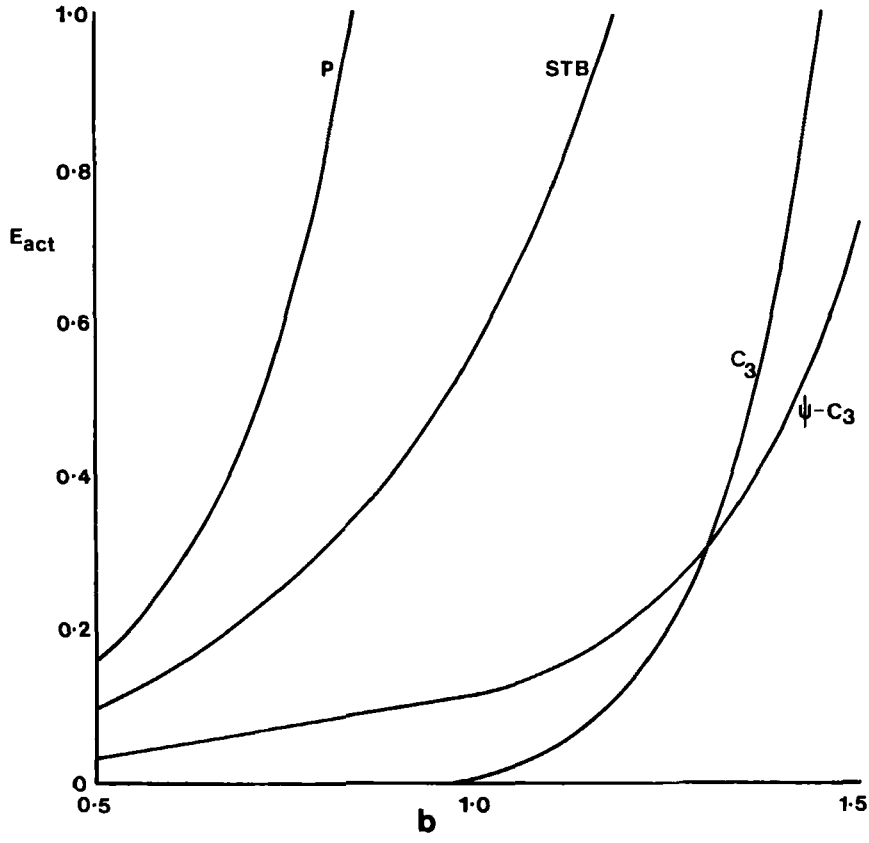

Fig. 18. Activation energies for racemization of tris(bidentate) complexes as a function of normalized bite b: C_3, trigonal twist about the C_3-axis; ψ-C_3, trigonal twist about a pseudo-C_3-axis, STB, skew-trapezoidal bipyramidal intermediate; P, planar intermediate.

proximately 1.3, the longer edges of the rectangle are those between the bidentate ligands, and the twist about the C_3-axis will be favored (Fig. 17*a*). For larger normalized bites the longer edges of the rectangle are those spanned by the bidentate ligands, and the second reaction will be favored (Fig. 17*b*).

The activation energy for these intramolecular twists are shown as a function of normalized bite in Fig. 18, calculated for $n = 6$. Similar curves are obtained for $n = 1$ and $n = 12$. Other possible reaction intermediates such as a skew-trapezoidal bipyramid (Fig. 19*a*; cf Section III.D.), or a planar hexagon (Fig. 19*b*) have considerably higher energies of activation (Fig. 18).

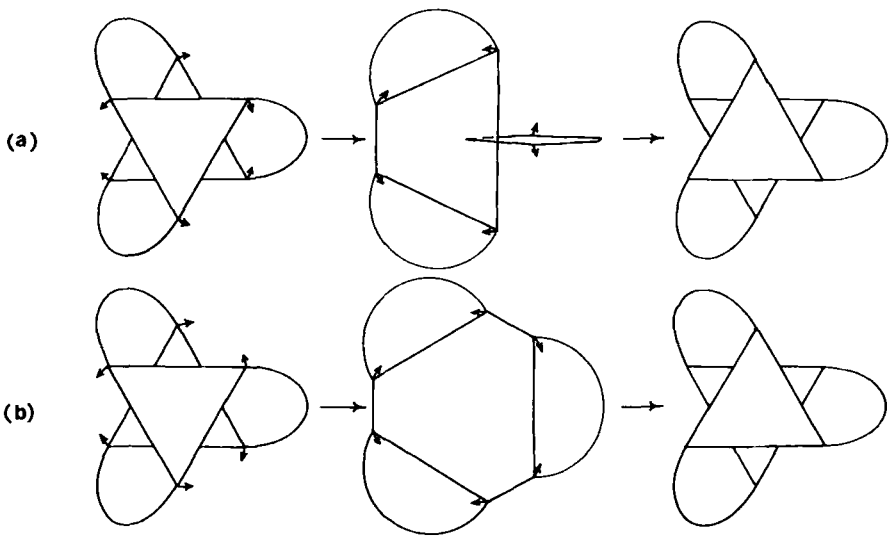

Fig. 19. Racemization of tris(bidentate) complexes: (*a*) skew-trapezoidal bipyramidal intermediate; (*b*) planar intermediate.

These intramolecular twists will inevitably be associated with some degree of bond stretching, and oversimplified conclusions based on the above geometric guidelines should be avoided. Electronic effects will also be important in transition-metal complexes.

Regardless of the proposed mechanism, it is clear from Fig. 18 that the activation energy will decrease as the normalized bite of the bidentate ligand decreases.

Three classes of complex that have been studied in detail are the dithiocarbamates, substituted tropolonates, and β-diketonates. These form four-, five-, and six-membered chelate rings, respectively (Fig. 20), with normalized bites of approximately 1.2, 1.3, and 1.4. It is generally observed that the rates of racemization via a trigonal twist mechanism are greater for the dithio-

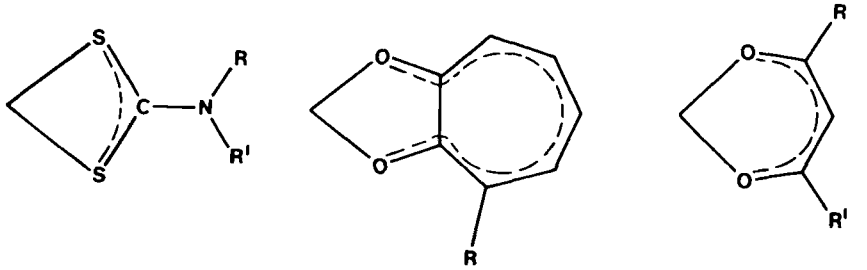

Fig. 20. Ring geometries in unsymmetrical dithiocarbamates, tropolonates, and β-diketonates.

carbamates (196) than for the tropolonates (58, 59), whereas trigonal twisting of the β-diketonate complexes is much slower, and isomerization generally occurs through a bond-breaking mechanism with five-coordinate intermediates. An exceptional case is cobalt(III), where the tris(tropolonate) complex unexpectedly racemizes more rapidly than the tris(dithiocarbamate) complexes.

Many tris(dithiocarbamates) are fluxional at room temperatures and have been studied in detail using ^{1}H-NMR techniques. For example, the ^{1}H-NMRsignals of iron(III) dithiocarbamates coalesce above approximately $-90°$. The activation energy for the high-spin $[Fe\{S_2CN(CH_2)_4\}_3]$ is ~ 31 kjoule mole^{-1}. However, the intermediate- and low-spin complexes have shorter Fe—S distances and larger normalized bites, and have higher activation energies as expected in the approximate range of 33 to 40 kjoule mole^{-1}.

Similarly, for substituted tropolonate complexes the activation energy for racemization decreases along the series $[Al(trop)_3]$ (~ 50 kjoule mole^{-1}) > $[Ga(trop)_3]$ (~ 40 kjoule mole^{-1}) > $[In(trop)_3]$ (~ 30 kjoule mole^{-1}) due to increasing metal–oxygen distances and decreasing normalized bites.

Similar intramolecular rearrangements are very rare for six-coordinate complexes containing only unidentate ligands and appear to be restricted to dihydrides of the type $[FeH_2(PR_3)_4]$ and $[RuH_2(PR_3)_4]$ (161) and to compounds of the type $[Os(SiMe_3)_2(CO)_4]$ (206).

K. Asymmetric Bidentate Ligands

Three equivalent asymmetric bidentate ligands can be incorporated into the repulsion energy calculations by specifying that the metal–ligand bond lengths to the two ends of each bidentate are given by unity and the bond-length ratio R, respectively. Two isomers are now possible. The first is the *facial*-isomer, in which the three fold axis of the coordination polyhedron is retained (Fig. 21*a*). The second isomer has no elements of symmetry and is the *meridional*-isomer (Fig. 21*b*).

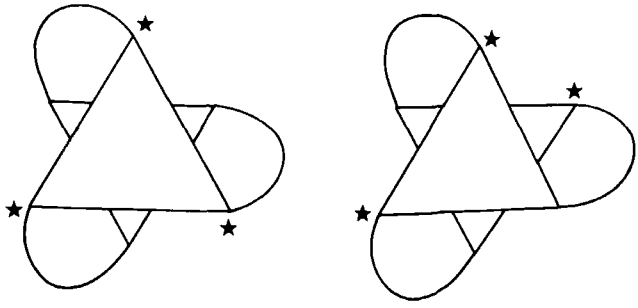

Fig. 21. *Facial*- and *meridional*-isomers of [M(asymmetric bidentate)$_3$]$^{x\pm}$.